Astronomy & Astrophysics

Stellar content of extremely red quiescent galaxies at *z* > 2

M. López-Corredoira[1,2], A. Vazdekis[1,2], C. M. Gutiérrez[1,2], and N. Castro-Rodríguez[3]

[1] Instituto de Astrofísica de Canarias, 38205 La Laguna, Tenerife, Spain
e-mail: martinlc@iac.es
[2] Departamento de Astrofísica, Universidad de La Laguna, 38206 La Laguna, Tenerife, Spain
[3] GRANTECAN S. A., 38712 Breña Baja, La Palma, Spain

ABSTRACT

Context. A set of 20 extremely red galaxies at $2.5 \leq z_{\rm phot.} \leq 3.8$ with photometric features of old passive-evolving galaxies without dust, with stellar masses of $\sim 10^{11}$ $M_\odot$, have colors that could be related to passive-evolving galaxies with mean ages larger than 1 Gyr. This suggests they have been formed, on average, when the Universe was very young (<1 Gyr).
Aims. We provide new estimates for the stellar content of these 20 galaxies, with a deeper analysis for two of them that includes spectroscopy.
Methods. We obtained, with the GRANTECAN-10.4 m, ultraviolet rest-frame spectra of two galaxies and analyzed them together with photometric data. The remaining 18 galaxies are analyzed only with photometry. We fit the data with models of a single-burst stellar population (SSP), combinations of two SSPs, as well as with extended star formation.
Results. Fits based on one SSP do not provide consistent results for the blue and red wavelengths. Moreover, the absence in the spectra of a break at $\sim 2 \times 10^3$ Å indicates that a rather young component is necessary. Using two SSPs we can match the photometric and spectroscopic data, with the bulk of the stellar population being very old (several Gyr) and the remaining contribution (<5% of stellar mass fraction) from a young, likely residual star formation component with age $\lesssim 0.1$ Gyr. Exponentially decaying extended star formation (τ) models improve slightly the fits with respect to the single burst model, but they are considerably worse than the two SSP based fits, further supporting the residual star formation scenario.
Conclusions. The fact that one SSP cannot match these early-type galaxies highlights the limitations for the use of age estimators based on single lines or breaks, such as the Balmer break used in cosmic chronometers, thus questioning this approach for cosmological purposes.

Key words. galaxies: evolution – galaxies: high-redshift – cosmology: observations

1. Introduction

Ages of quiescent galaxies have been derived by fitting photometric data with stellar population synthesis models since the pioneering works for low redshift galaxies of, for example, Tinsley (1980), and at redshifts larger than one since more than a decade ago. Early-type massive extremely red objects with $z \sim 1.4$ (e.g., Longhetti et al. 2005; Trujillo et al. 2006) have been found to be old. In fact, a galaxy at $z = 1.22$ has an average age of its stellar population of around 5.0 Gyr (Longhetti et al. 2005), within the limit of the age of the Universe at this redshift (5.3 Gyr). More distant ($z > 2$) red galaxies were analyzed (Labbé et al. 2005) with observations that provide rest-frame ultraviolet to infrared photometry (0.3–8.0 μm). These observations found that three out of 14 red galaxies were indeed old galaxies with mean luminosity-weighted ages of 2.6 Gyr at $z = 2.7$, 3.5 Gyr at $z = 2.3$, and 3.5 Gyr at $z = 2.3$ respectively, representative of the average age of the stellar populations. The age of the Universe in standard models at both redshifts of 2.7 and 2.3 is 2.5 Gyr and 3.0 Gyr respectively. These are mean luminosity-weighted ages assuming a single stellar population. Toft et al. (2005) fit synthesis models to spectra of red compact galaxies with ages 5.5, 3.5, and 1.7 Gyr for redshifts 1.2, 1.9, and 3.4 (ages of the Universe respectively: 5.4, 3.6, 2.0 Gyr), within the limit. Galaxies at very high redshift ($z \sim 4$) were analyzed (Rodighiero et al. 2007) to find, with optical, near-infrared and mid-infrared surveys, an important ratio of old ($\gtrsim 1$ Gyr) and massive ($\sim 10^{11}$ $M_\odot$) galaxies.

With similar techniques, evidence was presented for 11 massive and evolved (0.2–1.0 Gyr) galaxies at redshifts $4.9 \leq z_{\rm phot.} \leq 6.5$ (Wiklind et al. 2008). Therefore, it is clear that there are bright massive galaxies at $z > 2.5$ (e.g., Alcalde Pampliega et al. 2015). It is clear from this information that the formation of very massive elliptical galaxies takes place at very high redshifts. These tight limits to the age of the galaxies can be in principle used to constrain the age of the Universe at different redshifts, and consequently to constrain the cosmological models (e.g., Simon et al. 2005), although there are uncertainties such as those from the photometric redshifts or the fact that the age estimation should be understood in relative terms, especially when galaxies are very old (Age Zero Point issue; Vazdekis et al. 2001; Schiavon et al. 2002). The existence of very massive galaxies almost as old as the Universe is in tension with semianalytic ΛCDM models, which claim that these galaxies were assembled much later (Guo et al. 2011). This is what was called the impossible early galaxy problem, by which observations find, by several orders of magnitude, more very massive haloes at very high redshift than predicted, implying that these massive galaxies formed impossibly early (Steinhardt et al. 2016). This is along the line suggested by the "downsizing" scenario of galaxy formation in which most massive galaxies assembled important amounts of their stellar content rapidly (in 1–2 Gyr) beyond $z \sim 3$ in very intense star formation events (Pérez-González et al. 2008).

Another example of the exploration of the age of quiescent galaxies is given in the paper by Castro-Rodríguez & López-Corredoira (2012, hereafter CL12). Among a sample in the *XMM*-LSS field of ~60 thousand galaxies with deep photometry in the visible (Subaru telescope), near infrared (UKIDSS-Ultra Deep Survey) and mid infrared (IRAC), with redshifts derived photometrically, CL12 searched for extremely red galaxies at $z_{\rm phot.} \geq 2.5$ with photometric features of old passively evolving galaxies and without dust (see further details in Sect. 2.1). They prove to be massive galaxies (stellar masses of ~$10^{11} M_\odot$) which were formed on average when the Universe was very young (<1 Gyr), assuming the standard cosmological parameters (CL12) and one single-burst stellar population (SSP).

The problem becomes more complex if we bear in mind that these elliptical galaxies that host an old, virtually single, stellar population (Renzini 2006) may have a small residual component from young stellar populations, as observed in local galaxies (Vazdekis et al. 1997; Atlee et al. 2009). This is more relevant at high redshift because the optical range samples the ultraviolet (UV) at rest, and this range is particularly sensitive to the hottest stars of the youngest stellar population components. Determining such contributions is relevant for constraining the latest generation of cosmological hydro-dynamical simulations like EAGLE, which predict some small level of recent star formation (Trayford et al. 2015). This is a key aspect of the work presented here, as opposed to many studies that often assume one SSP, which are biased toward the youngest contributions for fitting their data, and therefore the maximum age of the oldest population of the galaxy may be underestimated. Deriving accurately the amount of young stellar populations in early-type galaxies is of paramount relevance to their formation within the ΛCDM model (e.g., Kaviraj et al. 2007) and particularly to constrain whether such contributions are consistent with residual star formation after an initial monolithic-like rapid formation phase (e.g., Oser et al. 2010), or in an extended formation assuming a delayed exponentially declining star formation history (Domínguez-Sánchez et al. 2016). Moreover, the fact that one SSP may not match these early-type galaxies highlights the limitations for the use of age estimators based on single lines or breaks, such as the Balmer break used in cosmic chronometers (Moresco et al. 2012, 2016), thus questioning this approach for cosmological purposes.

Here, we aim to perform a more accurate analysis of the stellar populations for the objects of the CL12 sample, modeling the photometry and spectra with one or two SSPs. There are studies of spectra in passively evolving galaxies up to $z \approx 2$ (e.g., McCarthy et al. 2004; Cimatti et al. 2004, 2008; Mignoli et al. 2005; Toft et al. 2012; Whitaker et al. 2013; Bedregal et al. 2013; Geier et al. 2013; Belli et al. 2015; Mendel et al. 2015; Onodera et al. 2015; Lonoce et al. 2015). The challenge here is to study low resolution spectra of faint galaxies ($m_R = 24$–25) dominated by absorption features at $z > 2$. We will also use the same photometric data used by CL12 for all of their 20 galaxies, and we will constrain the age and redshift of the galaxies with better accuracy. By means of very-low resolution spectra, we test further this result through a more accurate method for two of these galaxies, #40812 and #78891, with photometric redshifts determined by CL12 of $z = 2.57$ and $z = 2.71$ respectively. We will explore the spectral range from 5000 to 9000 Å, which at rest-frame covers the range around 2000 Å. That UV range has an abrupt break (see Fig. 9 of Bruzual & Charlot 2003, hereafter BC03) that depends strongly on the age of the stellar population, so these spectra can be useful for this purpose. The low

resolution spectra in this range allow us to fit the best template with its corresponding age. The metallicity effect will also be considered, whose effect in the change of the continuum of the spectra is smaller at such young ages.

Section 2 describes the photometric and spectroscopic data used in this paper. Section 3 describes two sets of stellar population synthesis models used here. The results of the best fit ages and other parameters for the two selected galaxies are given in Sects. 4–6. In Sect. 7, we do some similar analysis only with photometry for the remaining 18 galaxies of the list. Discussions and conclusions are presented in Sects. 8 and 9.

2. Data

2.1. High redshift sample

In CL12, the photometric selection was carried out with color-color diagrams similar to those of Pozzetti & Mannucci (2000) or Fang et al. (2009) in the visible/near-infrared, but shifted towards longer wavelengths. A negligible emission in 24 μm was also required to further reduce the chances of obtaining a star-burst in the selection. Moreover, CL12 selected objects for which the photometrically derived redshifts have been confirmed by different authors and different algorithms within $\frac{\Delta z}{(1+z)} < 0.1$. In total, CL12 obtained a sample of 20 galaxies with $2.5 \leq z_{\rm phot.} \leq 3.8$. From these galaxies, the rest ($B - V$) color was determined through spectral energy distribution (SED) using templates of galaxies with the software Interrest v2.0 (Taylor et al. 2009; López-Corredoira 2010). Average colors ($B-V$) between 0.7 and 0.8 (Vega calibration) were obtained. There is negligible extinction and reddening due to our Galaxy. From the comparison with a stellar population synthesis model and solving the degeneracy with metallicity by means of an iterative method which takes into account the mass-metallicity relationship (method developed by López-Corredoira 2010 using the models by Vazdekis et al. 1996), these colors could be related to ages above 1 Gyr of a stellar population in passive-evolving galaxies. We use two sets of data for two galaxies from the CL12 sample, numbers #40812 (RA = 2h16m42.40s, $\delta = -5°8'6.5''$) and #78891 (RA = 2h18m21.99s, $\delta = -4°46'49.4''$), corresponding to the number of sources in the Ultra Deep Survey *XMM*-LSS.

2.2. Photometric data

For these galaxies, we use the same photometric data as CL12, with the filters B, V, R, i, z, J, H, K, [3.6 μm], and [4.5 μm] (only for #40812). We correct the photometry of Galactic extinction, with $A_R = 0.047$ and $A_R = 0.045$ (Schlafly & Finkbeiner 2011) respectively for the galaxies #40812 and #78891. Similar photometric analysis will be done for the remaining 18 galaxies of CL12 in Sect. 7.

2.3. Spectroscopic data

Spectroscopic observations of the optical counterparts were made with the OSIRIS spectrograph on the 10.4 m GTC in La Palma (Canary islands, Spain) using its service observing mode on August 29 and 31 2014. Long-slit spectra of the R300R grism/binning 2×2 over the range 4800–10 000 Å were obtained, at the parallactic angle of each exposure, under 0.8–0.9″ seeing condition and a slit width of 1″. The total exposure time was 2670 s for galaxy #40812, and 8010 s for galaxy #78891. The spectral resolution with this configuration was 7.75 Å/pixel; but, in order to gain signal/noise ratio (S/N), we binned the spectrum in bins of three and ten pixels respectively for both galaxies,
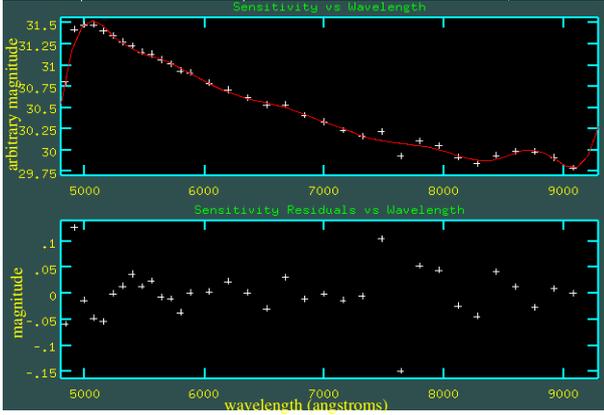
Fig. 1. Sensitivity versus wavelength in the flux calibration of spectra using the standard star Ross 640.

so finally we got spectra with resolutions of 23.26 Å/pixel and 77.35 Å/pixel respectively (with a redshift of 2.5; this is equivalent to 6.6 and 22.1 Å/pixel at rest), with average S/N of 3.0 and 2.2 respectively. The spectra were analyzed following the standard procedure using IRAF which comprises bias subtraction, flat-field correction, co-addition of the three single exposures, spectral extraction, wavelength calibration, and flux calibration. The spectroscopic standard star Ross 640 (Oke 1990) was observed for the spectrophotometric calibration in the two nights of the observations.

The accuracy of the flux calibration is important here because we will fit the shape of the continuum of the spectrum and not its lines, given the low S/N of the data. We only used the spectral region between 4980 and 8850 Å, where the transmission is high enough and allows an error of <5% in the flux absolute calibration, as estimated from possible variations in the way to extract the spectrum (with the command "apall" of IRAF) and the calibration with the standard star (with the commands "standard", "sensfunc", and "calibrate" of IRAF). We consider this error in the flux calibration negligible for the determination of the error of the parameters to be fitted in Sect. 4. In Fig. 1, we show the accuracy in the response calibration using the standard star Ross 640. The absolute flux calibration of the spectra was renormalized in order to fit their AB magnitudes in R: 23.60 and 24.89 respectively, and later corrected for Galactic extinction $A_\lambda \propto \lambda^{-1.4}$; $A_R = 0.047$ and $A_R = 0.045$ (Schlafly & Finkbeiner 2011) for the galaxies #40812 and #78891 respectively.

3. Models

3.1. BC03 model

The stellar population synthesis by BC03 (also called GALAXEV) computes the spectral evolution of stellar populations for ages between 10^5 and 2×10^{10} yr at a resolution of 3 Å along the wavelength range from 3200 to 9500 Å for a range of metallicities [Z/H] between –0.40 and 0.40. These predictions are based on the observed stellar library STELIB (Le Borgne et al. 2003), which allows a reasonable coverage of metallicities around solar. It also computes the spectral evolution across a larger wavelength range, from 91 Å to 160 μm, at lower resolution using theoretical stellar spectra. Padova 1994 evolutionary tracks (Bertelli et al. 1994) and Chabrier (2003) IMF (initial mass function) were used. The model incorporates all the stellar evolutionary phases and reproduces well the

observed optical and near-infrared color-magnitude diagrams of Galactic star clusters of various ages and metallicities, and typical galaxy spectra from the early data release (EDR) of the Sloan Digital Sky Survey (SDSS; see BC03 for more details). Here we use the 30 templates (ten ages, three metallicities) of instantaneous-burst models used by Tremonti (2003) to fit the continua in SDSS galaxy spectra.

3.2. E-MILES

We also use the UV-extended E-MILES models, which cover the spectral range $\lambda\lambda$ 1680–50 000 Å at moderately high resolution. The models employ the Hubble's NGSL (Next Generation Spectral Library) space-based stellar library (Gregg et al. 2006), as prepared in Koleva & Vazdekis (2012), to compute spectra of single-age, single-metallicity stellar populations blueward of 3540 Å. Other empirical stellar spectral libraries are employed for redder wavelengths (Röck et al. 2016). The models span the metallicity range $-1.79 \leq$ [M/H] $\leq +0.26$ for ages larger than 30 Myr, for a suite of IMF types with varying slopes. These models provide reasonably good fits to the integrated colors and most line-strengths of nearby early-type galaxies with different masses (Vazdekis et al. 2016). In the relevant rest-frame spectral range the resolution of these models is $FWHM = 3$ Å.

3.3. TP-AGB effect

We do not take into account the enhanced contributions from thermally pulsing asymptotic giant branch (TP-AGB) stars, as done by some authors (e.g., Maraston 2005; Bruzual 2007). For old stellar components ($\gtrsim 1$ Gyr), the contribution from this evolutionary phase is fading as the red giant branch is developing rapidly; moreover, the rest-frame spectral range of our reddest filter does not extend significantly beyond 1 μm. For the young populations (a few hundred Myr), the flux is dominated by UV light and it has small contribution from near-infrared wavelengths at rest, but the evolutionary phase of TP-AGB stars has no impact on the UV spectral range. Therefore, we consider this effect as a minor correction that will not alter significantly the results of this paper.

4. Fitting of parameters with a single stellar population

Either with E-MILES or BC03, we have a set of normalized spectra that depend on the age and metallicity of the represented quiescent galaxy: $L^{\text{E-MILES/BC03}}(\text{age}, [\text{M/H}]; \lambda_{\text{rest}})$. If the galaxy is at redshift z, the corresponding observed flux would be

$$F^{\text{E-MILES/BC03}}(\text{age}, [\text{M/H}], z; \lambda) = \tag{1}$$

$$\frac{L_0 L^{\text{E-MILES/BC03}}(\text{age}, [\text{M/H}]; \lambda/(1+z))}{4\pi d_L(z)^2(1+z)},$$

where $d_L(z)$ is the luminosity distance corresponding to a redshift z with a standard cosmology of $\Omega_m = 0.3$, $\Omega_\Lambda = 0.7$, $H_0 = 70$ km s^{-1}/Mpc.

With our spectra and photometric data, we fit the free parameters age, [M/H], z, and the amplitude L_0 by minimizing the reduced chi-square,

$$\chi^2_{\text{red}} = \frac{1}{N_{\text{d.o.f.}}} \sum_{i=1}^{N} \frac{[F_{\text{obs.}}(\lambda_i) - F^{\text{E-MILES/BC03}}(\text{age}, [\text{M/H}], z; \lambda_i)]^2}{\sigma^2(\lambda_i)},$$

$$\tag{2}$$

Table 1. Best fit parameters obtained with a single stellar population for galaxies #40812 and #78891 combining spectroscopy and photometry.

Galaxy	Model	$\chi^2_{\rm red.}$	z	Age (Gyr)	[M/H]
#40812	E-MILES	3.69	$3.10^{+0.20}_{-0.20}$	$1.00^{+0.75}_{-0.10}$	$-1.26^{+0.30}_{-1.01}$
#40812	BC03	9.51	$2.40^{+0.10}_{-0.10}$	$0.29^{+0.34}_{-0.19}$	$-0.40^{+0.40}_{-0}$
#78891	E-MILES	1.07	$3.20^{+0.25}_{-0.70}$	$1.75^{+1.00}_{-1.25}$	$-1.79^{+1.54}_{-0.48}$
#78891	BC03	3.33	$2.45^{+0.15}_{-0.15}$	$0.29^{+0.34}_{-0.19}$	-0.4, unconstr.

where $N_{\rm dof} = N - \nu$ is the number of degrees of freedom for ν free parameters (in our case here, $\nu = 4$); N is the number of available points λ_i, both in spectroscopy and photometry. The σ_i is the error bar of the data: it is available for the photometry and calculated for the spectra (we take for all pixels the same $\sigma(\lambda_i)$) of 3.5×10^{-19} and 1.5×10^{-19} erg/s/cm^2/Å for the binned spectra of galaxies #40812 and #78891, which correspond to the average S/N of 3.0 and 2.2 measured in these spectra per pixel). We constrain the range of redshifts to be $z > 0.5$, which is reasonable given our previous measuments of the photometric redshifts. The values of $F^{\rm E-MILES/BC03}$ which correspond to the observed λ_i are obtained by binning and interpolating the model in the case of spectra, or by convolving the spectra of the theoretical model with the transmission curves corresponding to the broad-band filters for which the photometry was carried out.

Once we get the free parameters that minimize the previous expression in Eq. (2), their error bars are derived by constraining the models that follow $\chi^2_{\rm red} < \chi^2_{\rm red,minimum}\left[1 + \frac{f(\rm CL)}{N_{\rm dof}}\right]$ with $f(\rm CL) = 4.7$ for 68.3 CL (1σ) and $f(\rm CL) = 9.7$ for 95.4 CL (2σ), taking into account that we use four free parameters (Avni 1976). The fact that we have included a factor $\chi^2_{\rm red,minimum}$ in the right hand of the inequality is to take into account that in cases with $\chi^2_{\rm red,minimum} \neq 1$ the errors were underestimated or overestimated; that is, this is equivalent to assuming that our fit is a "good fit" (with $\chi^2_{\rm red,minimum} \approx 1$) and multiplying the error bars by some factor to get it. BC03 has the advantage of using the whole spectrum range and photometric data, whereas E-MILES models are constrained in a more limited wavelength range in the UV with $\lambda_{\rm rest} > 1680$ Å.

4.1. Results

The results for the two galaxies for which we obtained the spectra are given in Table 1 and in Figs. 2 and 3. The metallicities are almost without constraint from the fits, which indicates that the shape of the spectra is more sensitive to the age than to the metallicity, as expected in this age regime. There are no big breaks around 2000 Å, which indicates that the galaxies cannot be too old (a galaxy with 2 Gyr would produce a conspicuous break, which is not observed here; although there is some dispersion among the results for the redshift and age of the galaxies with the different fits, they are roughly compatible with each other.

The ages correspond to an intermediate age population. By averaging the results of both models (the data are not independent so the error bars are not reduced proportionally to $\sqrt{N}$ by combining N data), we obtain $0.90^{+0.10}_{-0.12}$ Gyr and $0.37^{+0.48}_{-0.30}$ Gyr respectively for galaxies #40812 and #78891.

With the same kind of combination, the most likely redshifts are 2.54 ± 0.12 for galaxy #40812 and 2.48 ± 0.21 for galaxy #78891. Other photometric redshifts have been published: for galaxy #40812: $z = 2.57$ (CL12), $z = 2.63$ (Rowan-Robinson et al. 2008), $z = 2.16$ (Rowan-Robinson et al. 2013), $z = 2.53$ (Williams et al. 2009); for galaxy #78891: $z = 2.71$ (CL12), $z = 2.38$ (Rowan Robinson et al. 2008), $z = 2.23$ (Rowan-Robinson et al. 2013), $z = 2.94$ (Williams et al. 2009). They are roughly compatible with our results here, provided that we allow a generous error bar for these numbers (up to 20%).

Nonetheless, the fits with single stellar population for the range of photometric and spectroscopic data are not good. Only the fit with E-MILES to galaxy #78891 is good because it finds a solution at high z compatible with the highest wavelength data, but this solution fails again when we extend the data to the far UV region using the BC03 models. We see that it is not possible to reconcile both the infrared photometry with the ultraviolet data: a good fit to the shortest wavelengths does necessarily lead to a flux prediction which is too low in the mid-infrared. This denotes that the galaxies are either more complex than quiescent galaxies with a single episode of stellar formation, or that there is some non-negligible extinction. We will explore these two scenarios in the following sections.

4.2. Adding extinction

In our fits, we have assumed that our galaxies are dust free following the CL12 selection based both on color-color diagnostic and on low 24 μm emission. At 2175 Å at rest, we do not see any bump in the spectra, which would be characteristic of a significant extinction in a Milky Way-like object. We tested whether the bad fits obtained with the BC03 model using only one SSP could be improved if we allow some internal extinction in our galaxies. As we have seen that metallicity does not play an important role in fits, we substitute it with a new free parameter: the internal extinction normalized in V at-rest $A_{V,{\rm int}}$. In this case we use the value of metallicity of the previous fit. For the extinction law, we use an attenuation curve often used in high-redshift studies: the law derived by Calzetti et al. (2000), derived empirically for a sample of nearby starburst (SB) galaxies. The 2175 Å bump is absent for this law: this characteristic suggests that starburst galaxies contain small magellanic cloud-like dust grains rather than Milky Way-like grains. The application of this law is suggested for the central star-forming regions of galaxies, and therefore is appropriate for high-z galaxies. For this reason, Calzetti's law is used to correct the value of the SFR at high-redshift, and we use this extinction law here, with the parameter $R_V = 4.05$. Then, we perform our fit with three free parameters, z, age, and $A_{V,{\rm int}}$, for the case of the fit of #40812 with BC03 model with fixed [M/H] $= -0.4$. The best fit is obtained for $z = 2.40$, age $= 0.29$ Gyr, and $A_{V,{\rm int}} = 0.035$, getting a $\chi^2_{\rm red.} = 9.47$, not much better than the fit without extinction and free metallicity (which provided $\chi^2_{\rm red.} = 9.51$); this is illustrated in Fig. 2. We conclude that the obtained mismatch cannot be attributed to internal extinction in the galaxies.

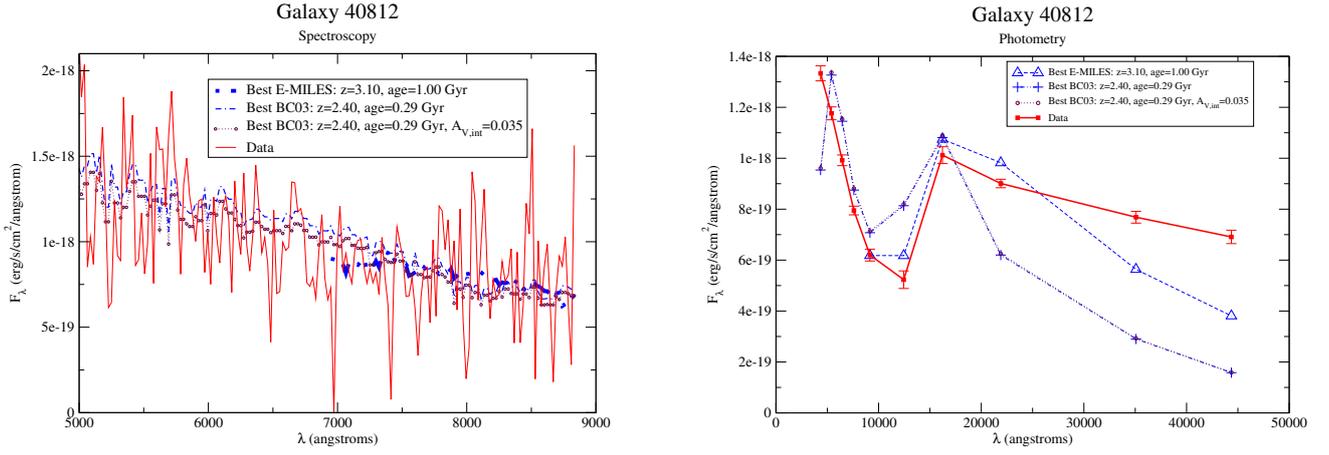Galaxy 40812
Spectroscopy

Galaxy 40812
Photometry

Fig. 2. Analysis of galaxy #40812: best fits to the combination of spectrum and photometric data obtained with the E-MILES, BC03, and BC03 with internal extinction. *Left*: spectrum. *Right*: photometry.
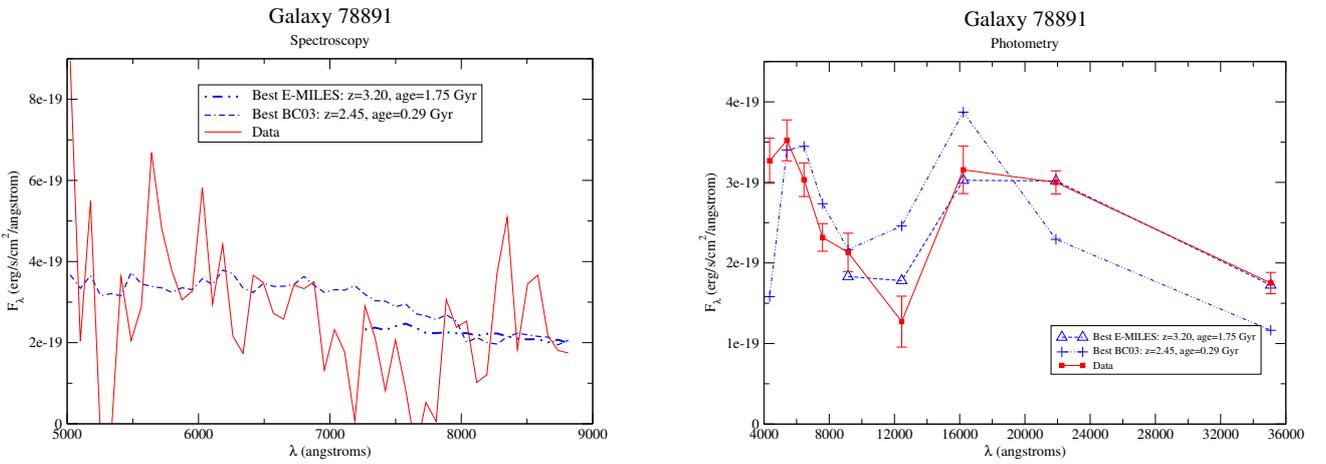
Galaxy 78891
Spectroscopy

Galaxy 78891
Photometry

Fig. 3. Analysis of galaxy #78891: best fits to the combination of spectrum and photometric data obtained with the E-MILES and BC03. *Left*: spectrum. *Right*: photometry.

5. Fitting of parameters with two single stellar populations

Here we perform the fits using two single stellar populations (SSPs), one of them relatively old and another one young. We allow five free parameters, apart from the amplitude: the redshift (z), the ratio of old/young population (A_2), the age of the young population age_1 (constrained to be less than 0.3 Gyr), the age of the old population age_2, and the metallicity [M/H] (the same for both populations; indeed for the younger component it is not important what the metallicity is because the models are almost completely insensitive to it). For $\nu = 6$ free parameters, $f(\mathrm{CL}) = 7.0$ for 1σ or 12.8 for 2σ.

$$F^{\mathrm{BC03/E-MILES}}(age_2, A_2, z; \lambda) = \qquad (3)$$

$$\frac{L_0 L^{\mathrm{BC03/E-MILES}}(age_1, [\mathrm{M/H}]; \lambda/(1+z))}{4\pi d_L(z)^2 (1+z)}$$

$$+ \frac{A_2 L_0 L^{\mathrm{BC03/E-MILES}}(age_2, [\mathrm{M/H}]; \lambda/(1+z))}{4\pi d_L(z)^2 (1+z)}.$$

The normalization of the spectra is such that $L^{\mathrm{BC03/E-MILES}}(\lambda = 5500$ Å$) = 1$. This means that A_2 represents the ratio of old/young luminosity at 5500 Å at rest. The result of the fits for both galaxies is given in Table 2 and in Figs. 4–6.

The fits with two SSPs are much better (they have lower average reduced χ^2), especially when using the BC03 model, which allows us to see that the far UV, $\lambda_{\mathrm{rest}} < 1680$ Å, cannot be fitted simultaneously with the mid-infrared data for a single stellar population. It is clear that at least two components are necessary.

The plausibility of this second solution with two SSPs may be related to the possibility that these galaxies are experiencing some starbursts. In principle, our galaxies were selected to be passively evolving without dust and without starbursts, but we may wonder whether a very small number of young stars is possible. The ratio of young to old stellar masses can be calculated for the luminosity ratios A_2 and using the mass-luminosity ratio (Vazdekis et al. 2016, assuming Kroupa Universal IMF) at a wavelength of 5500 Å. They are given in Table 2. In all cases, the young stellar mass is less than 5% of the old stellar mass. This is compatible with the fact that they are elliptical galaxies dominated in mass by an old population. The average redshifts with two SSPs (combining MILES and BC03 results) are 2.69 ± 0.15 and 2.72 ± 0.28, similar to the redshifts obtained with one SSP.

Again, as stated in Sect. 4.2, we can test whether a modest amount of internal extinction in the galaxies, associated to the young population, may alter significantly the results. The fact that the young population fits the ultraviolet part very well without internal extinction correction indicates that we may most likely neglect extinction at all wavelengths. A small amount of

Table 2. Best fitted parameters with two stellar populations for galaxies #40812 and #78891.

Galaxy	Model	$\chi^2_{\rm red.}$	z	Age$_1$ (Gyr)	Age$_2$ (Gyr)	A_2	[M/H]	Young/old stellar mass
#40812	E-MILES	0.82	$2.55^{+0.25}_{-0.10}$	$0.07^{+0.02}_{-0.01}$	$14^{+0}_{-3.5}$	$2.0^{+0.2}_{-0.4}$	$+0.40^{+0}_{-0.14}$	$0.042^{+0.013}_{-0.010}$
#40812	BC03	1.41	$2.75^{+0.10}_{-0.10}$	$0.025^{+0.075}_{-0.020}$	$1.4^{+3.6}_{-0.5}$	10^{+1}_{-2}	$+0.40^{+0}_{-0.40}$	$0.009^{+0.008}_{-0.009}$
#78891	E-MILES	0.83	$2.35^{+0.60}_{-0.20}$	$0.04^{+0.26}_{-0.04}$	13^{+1}_{-12}	$2.8^{+7.2}_{-0.4}$	$+0.15^{+0.25}_{-1.64}$	$0.005^{+0.014}_{-0.005}$
#78891	BC03	1.34	$2.95^{+0.05}_{-0.25}$	$0.025^{+0.265}_{-0.020}$	$0.64^{+0.76}_{-0.35}$	12^{+4}_{-3}	+0.4, unconstr.	$0.014^{+0.035}_{-0.014}$
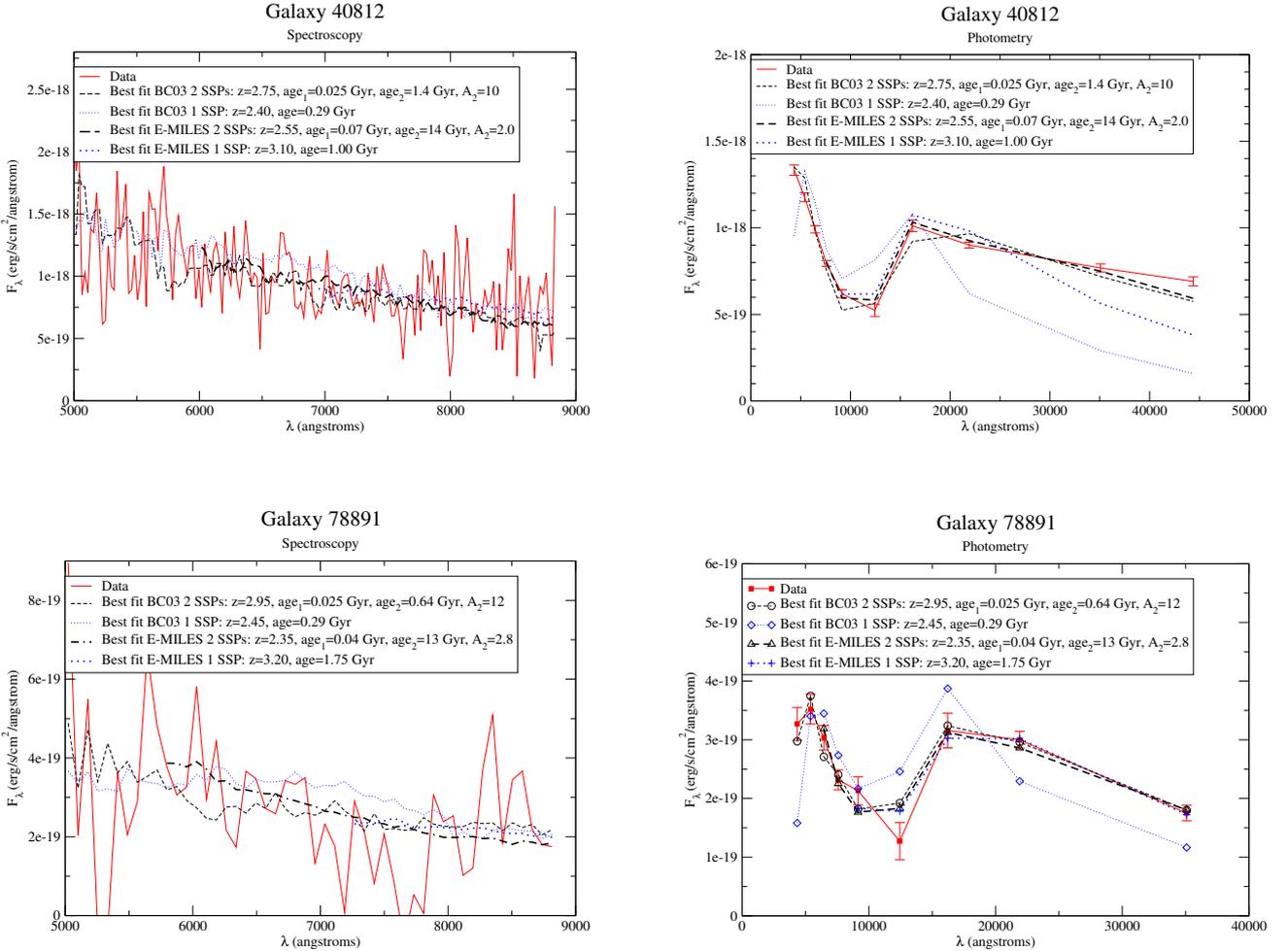
Fig. 4. Spectrum and photometry at observed wavelength corresponding to the best fits with two SSPs (see Table 2) or with one SSP (see Table 1) of spectroscopy or photometry for galaxies #40812 and #78891.

extinction might affect slightly the young population but has a negligible impact on the old population that dominates the reddest wavelengths.

To test these effects, we carried out again the fit of galaxy #40812 using the BC03 model (which reaches shorter wavelengths in the UV, thus allowing us to be more restrictive in the extinction magnitude), for three values of internal extinction, $A_{V,\rm int} = 0.02, 0.04, 0.08$, using again Calzetti et al. (2000)'s extinction law. The result is: $\chi^2_{\rm red.} = 1.43, 1.48$, and 1.65 respectively, slightly worse than 1.41 without extinction, and with similar values of the parameters for the best fits. The best fit is obtained without extinction and, even for a small amount of reddening, it does not alter our results.

6. Fit with extended star formation

We also tried another approach for fitting the data, which consists of an exponentially decaying star formation (τ model, as used by other authors, e.g., Sánchez-Domínguez et al. 2016). We may model the global spectral energy distribution as:

$$L(\lambda_{\rm rest}) = L_0 \int_0^{\rm age} {\rm d}t\, L_*(t, [M/H]; \lambda_{\rm rest}) e^{-\frac{{\rm age}-t}{\tau}}, \qquad (4)$$

where L_* is the luminosity per unit mass; we only use E-MILES this time, given that it has a higher resolution of ages. We discretize the integral into a sum of the different available components. A fit of this type, with z, age, [M/H], and τ as
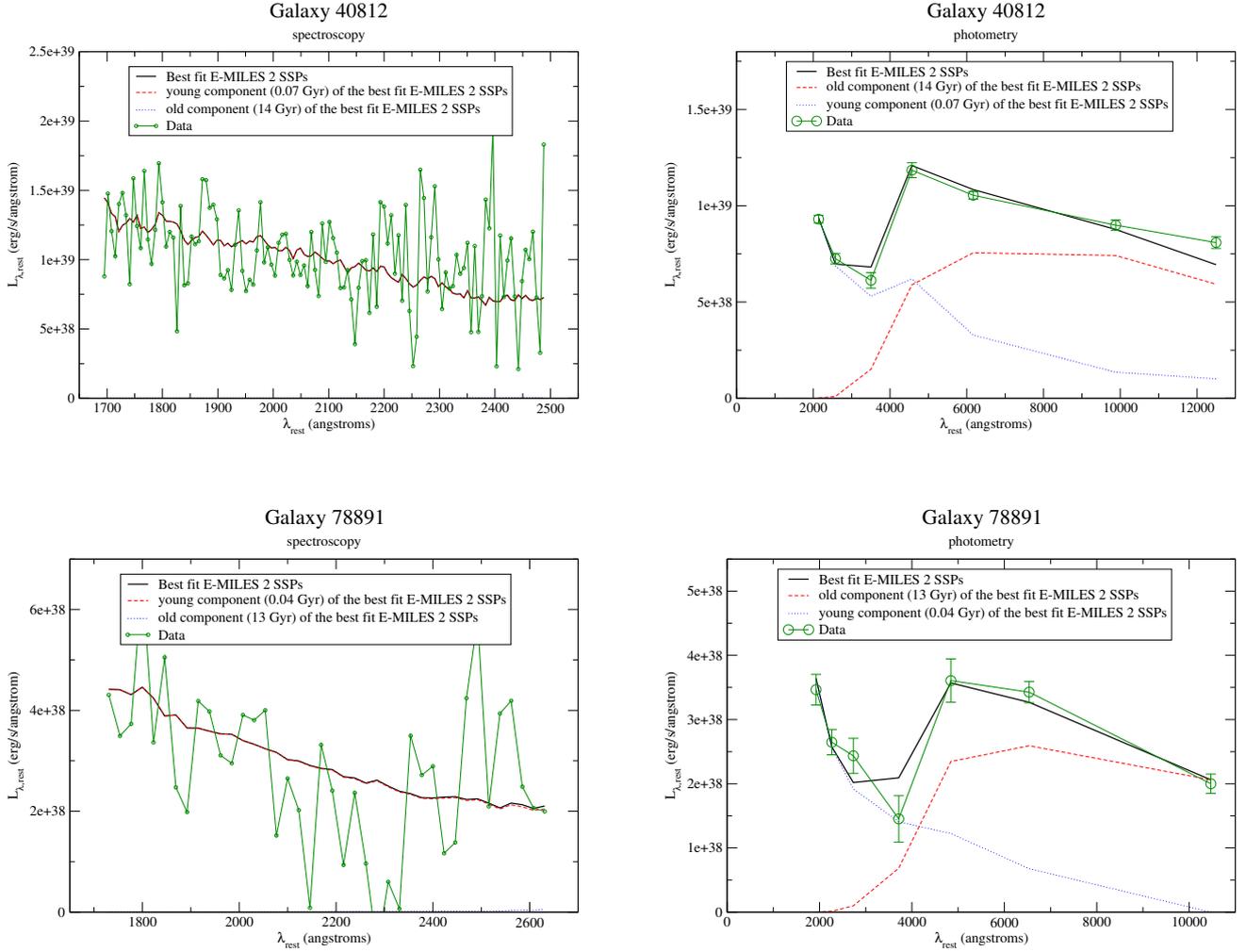
Fig. 5. Spectrum and photometry at rest corresponding to the best fits with two SSPs of E-MILES model (see Table 2) of spectroscopy or photometry for galaxies #40812 and #78891, indicating the decomposition of the young and the old component.

free parameters gives: for #40812, $\chi^2_{\rm red} = 2.62$, $z = 3.00^{+0.20}_{-0.10}$, age $= 11.5^{+2.5}_{-4.5}$ Gyr, $\tau = \infty$ (unconstrained within 1σ) (constant star formation rate), [M/H] $= -0.35$ (unconstrained within 1σ); for #78891, $\chi^2_{\rm red} = 1.02$, $z = 2.75^{-0.25}_{+0.45}$, age $= 14.0^{+0}_{-11.5}$ Gyr, $\tau = 160$ Gyr (unconstrained with 1σ) (almost constant star formation rate), [M/H] $= -0.66$ (unconstrained with 1σ). It is remarkable that the best fits obtained here are worse than those achieved with two SSPs ($\chi^2_{\rm red.} \geq 20\%$ larger), although better than with one SSP ($\chi^2_{\rm red.} \geq 30\%$ smaller). We conclude that the model with two SSPs is a better representation of the data, which further supports the residual star formation scenario.

7. Fitting the other 18 galaxies with 2 SSPs using only photometry

Table 1[1] of CL12 gives a list of 20 galaxies classified as extremely red objects and old galaxies. We have analyzed two of them in this paper with spectroscopic and photometric data. For the remaining 18 galaxies we only have photometric data. We showed in Sect. 5 that photometry alone shows the need for two

SSPs to produce a good fit. Therefore in this section we perform the fits of these 18 galaxies relying only on their photometric data. Here we only use the BC03 model, since we have seen that both E-MILES and BC03 give similar results, and BC03 has the advantage over E-MILES of including the wavelength range $\lambda_{\rm rest} < 1680$ Å. Applying the same fits as in Sect. 5 but only with photometry, we get the results given in Table 3 and Fig. A.1.

The analysis of these 18 galaxies gives similar results to those obtained for the two galaxies studied in the previous sections of this paper: a combination of a young (0.005–0.29 Gyr) and an old (0.64–11 Gyr) component gives an acceptable fit to our data in most cases. These results show that this star formation pattern is common to most of the galaxies studied here. The values of $\chi^2_{\rm red}$ are higher than the analysis with spectra+photometry because the relative photometric errors are much smaller than the spectroscopic ones. The old population dominates the red-near infrared range at rest, whereas the young population dominates the UV at rest. The obtained redshifts fall in all cases within the range 2.3–3.9, as expected. The metallicities are unconstrained because large variations of metallicity do not strongly change the predictions of the models.

For 11 of the 18 galaxies (those with numbers 1559, 10 585, 11 488, 14 598, 25 371, 26 888, 28 153, 28 841, 39 991, 79 102, and 85 772) we observe that the photometric data have the typical V-shaped pattern with minima around $\lambda_{\rm rest} \approx 3000$ Å,

---

[1] There is an error in Table 1 of that paper, as Cols. 5 and 6 were disordered and did not match the information of the galaxies in the first four columns. The corrected Table 1 is at: http://cdsads.u-strasbg.fr/NOTES/2012A+A...537A..31C.html

Table 3. Best fitted parameters with two stellar populations for the 20 galaxies of the CL12 list, first column indicating the number of source in the ultra deep survey *XMM*-LSS, except #40812 and #78891, using only photometry and the BC03 model.

Galaxy	$\chi^2_{\rm red.}$	z	Age$_1$ (Gyr)	Age$_2$ (Gyr)	A_2	[M/H]
#1559	2.13	$2.3^{+1.4}_{-1.0}$	$0.10^{+0.19}_{-0.095}$	$5^{+6}_{-4.1}$	$3.5^{+9.0}_{-1.5}$	+0.4, unconstr.
#6165	0.83	$2.4^{+0.4}_{-0.6}$	$0.29^{+0}_{-0.265}$	$1.4^{+9.6}_{-0.8}$	7^{+19}_{-4}	+0.4, unconstr.
#8303	0.19	$2.7^{+0.2}_{-0.2}$	$0.29^{+0}_{-0.19}$	$2.5^{+2.5}_{-0.9}$	$2.2^{+0.6}_{-0.4}$	$+0.4^{+0}_{-0.4}$
#10585	2.07	$2.5^{+1.0}_{-0.4}$	$0.10^{+0.19}_{-0.075}$	$11^{+0}_{-9.6}$	$3.5^{+6.5}_{-1.0}$	+0.4, unconstr.
#11488	2.91	$2.5^{+1.0}_{-0.4}$	$0.10^{+0.19}_{-0.075}$	$2.5^{+8.5}_{-1.9}$	$4.5^{+7.5}_{-4.0}$	+0.4, unconstr.
#14598	9.40	$3.1^{+0.6}_{-0.8}$	$0.10^{+0.19}_{-0.095}$	$0.9^{+10.1}_{-0.875}$	$2.4^{+7.6}_{-2.4}$	-0.4, unconstr.
#24756	6.71	$2.5^{+1.0}_{-0.6}$	$0.29^{+0}_{-0.265}$	$11^{+0}_{-10.71}$	$3.2^{+6.8}_{-2.8}$	0, unconstr.
#25371	2.18	$2.3^{+1.2}_{-0.6}$	$0.10^{+0.19}_{-0.075}$	$2.5^{+8.5}_{-1.9}$	$2.8^{+5.4}_{-2.4}$	+0.4, unconstr.
#26888	2.05	$3.1^{+0.8}_{-1.2}$	$0.10^{+0.19}_{-0.095}$	$11^{+0}_{-10.7}$	$8.0^{+17.5}_{-5.5}$	–0.4, unconstr.
#28153	3.92	$2.5^{+0.8}_{-0.4}$	$0.10^{+0.19}_{-0.075}$	$5^{+6}_{-4.1}$	$4.0^{+5.0}_{-3.0}$	+0.4, unconstr.
#28841	2.85	$3.3^{+0.8}_{-1.0}$	$0.10^{+0.19}_{-0.10}$	$2.5^{+8.5}_{-2.2}$	$6.5^{+19}_{-5.5}$	–0.4, unconstr.
#39991	9.06	$2.9^{+0.6}_{-0.8}$	$0.10^{+0.19}_{-0.095}$	$0.9^{+10.1}_{-0.8}$	$6.0^{+19.5}_{-6.0}$	–0.4, unconstr.
#44569	0.51	$2.9^{+0.2}_{-0.4}$	$0.29^{+0}_{-0.19}$	$5^{+6}_{-3.6}$	$1.0^{+0.8}_{-0.3}$	+0.4, unconstr.
#51547	1.90	$2.7^{+0.8}_{-0.6}$	$0.29^{+0}_{-0.265}$	$2.5^{+8.5}_{-1.9}$	$3.4^{+6.8}_{-2.8}$	0, unconstr.
#65143	6.71	$2.5^{+1.0}_{-0.6}$	$0.29^{+0}_{-0.265}$	$11^{+0}_{-10.7}$	$3.2^{+7.0}_{-2.8}$	0, unconstr.
#79102	5.69	$2.5^{+1.2}_{-1.2}$	$0.10^{+0.19}_{-0.095}$	$11^{+0}_{-10.4}$	$2.6^{+7.6}_{-1.8}$	+0.4, unconstr.
#85772	0.93	$3.1^{+0.6}_{-0.8}$	$0.10^{+0.19}_{-0.095}$	$5^{+6}_{-4.4}$	$8.5^{+17.0}_{-5.0}$	–0.4, unconstr.
#93574	3.63	$3.9^{+1.0}_{-2.6}$	$0.005^{+0.020}_{-0}$	$0.64^{+10.36}_{-0.54}$	$68^{+\infty}_{-68}$	–0.4, unconstr.

and decrease of flux over 6000 Å at rest. This pattern, which cannot be fully matched with a single SSP, can only be reproduced with two SSPs, as shown in Sect. 5. This shows that our two galaxies #40812 and #78891 analyzed previously are not peculiar cases in their stellar content.

8. Discussion on the age determination

8.1. The oldest age problem and systematic errors in the age that have not been taken into account

Surprisingly, our fits in Sect. 5 provide some solutions involving ages for the old component older than the Universe: the best fits with E-MILES for galaxies #40812 and #78891 give 14 Gyr and 13 Gyr respectively, although in the second case it is compatible with the age of the Universe within the error bars. Nonetheless, we must bear in mind that our assumptions (only two stellar populations, without dust, neglecting the light contamination from other galaxies, neglecting the TP-AGB uncertainty at $\lambda_{\rm rest} > 7000$ Å, or the assumption of a standard IMF) are only approximations, so there may be additional systematic errors attributed. Furthermore, in light of the recent evidence for a bottom-heavy IMF in massive early-type galaxies (La Barbera et al. 2013), the oldest component of our fits might be approached by such dwarf-enriched-IMF that redden the spectra by ~0.1 mag, which is equivalent to the change of slope between 3 and 10 Gyr (Vazdekis et al. 2012). Therefore, we cannot use the present result to establish firmly that we have found a galaxy older than the Universe, although certainly it is a very old galaxy. In fact, the analysis with the model BC03, which comprises the far UV part, gives an age of $1.4^{+3.6}_{-0.5}$ Gyr for galaxy #40812, which is compatible with the age of the Universe. Other independent estimators of age for the oldest population are necessary. We note that the oldest population dominates in the reddest wavelengths, so the estimator would be better if it is based on mid infrared observations ($\lesssim 5\ \mu$m, since the dust emission, although low, may become important over this wavelength; da Cunha et al. 2008, Fig. 5).

For the age of the oldest population in the remaining 18 galaxies analyzed in Sect. 7, we cannot set a good constraint. There are nine galaxies whose older stellar population components have best fit ages larger than 3 Gyr, but also lower values are allowed within errors. For the remaining nine galaxies, the best fits for the oldest component are between 0.5–3 Gyr and much lower ages are also allowed within the error bars.

The fact that half of the 20 galaxies of CL12 are better fitted with very high ages (≥ 3 Gyr) is due to the low slope in the spectra of the red-near infrared range at rest, which is almost flat in some cases. Younger populations of the oldest component require a larger value of $-\frac{{\rm d}L_\lambda}{{\rm d}\lambda}$ at $\lambda_{\rm rest} > 6000$ Å. Although we do not know why the reddest filters are providing such high fluxes, it is clear that the decrease in flux is milder in comparison to that expected for stellar populations with ages 1–2 Gyr.

8.2. On the unsuitability of cosmic chronometer methods

Some age-sensitive breaks like the Balmer one at 4000 Å at rest are contributed by similar light fractions from the two components (see Fig. 5, left) so they cannot serve as a direct indicator of the age of the oldest population, but instead can indicate an average age of the young and the old population. For instance, if the old population were 4.0 Gyr old and the young population were 0.1 Gyr old, with [M/H] = 0 both, the Balmer break $D_{4000} \equiv \frac{\overline{F}_\lambda(4050-4100\ \text{Å})}{\overline{F}_\lambda(3900-3950\ \text{Å})}$ would be 2.1 and 1.2 respectively for both populations (using E-MILES model; see
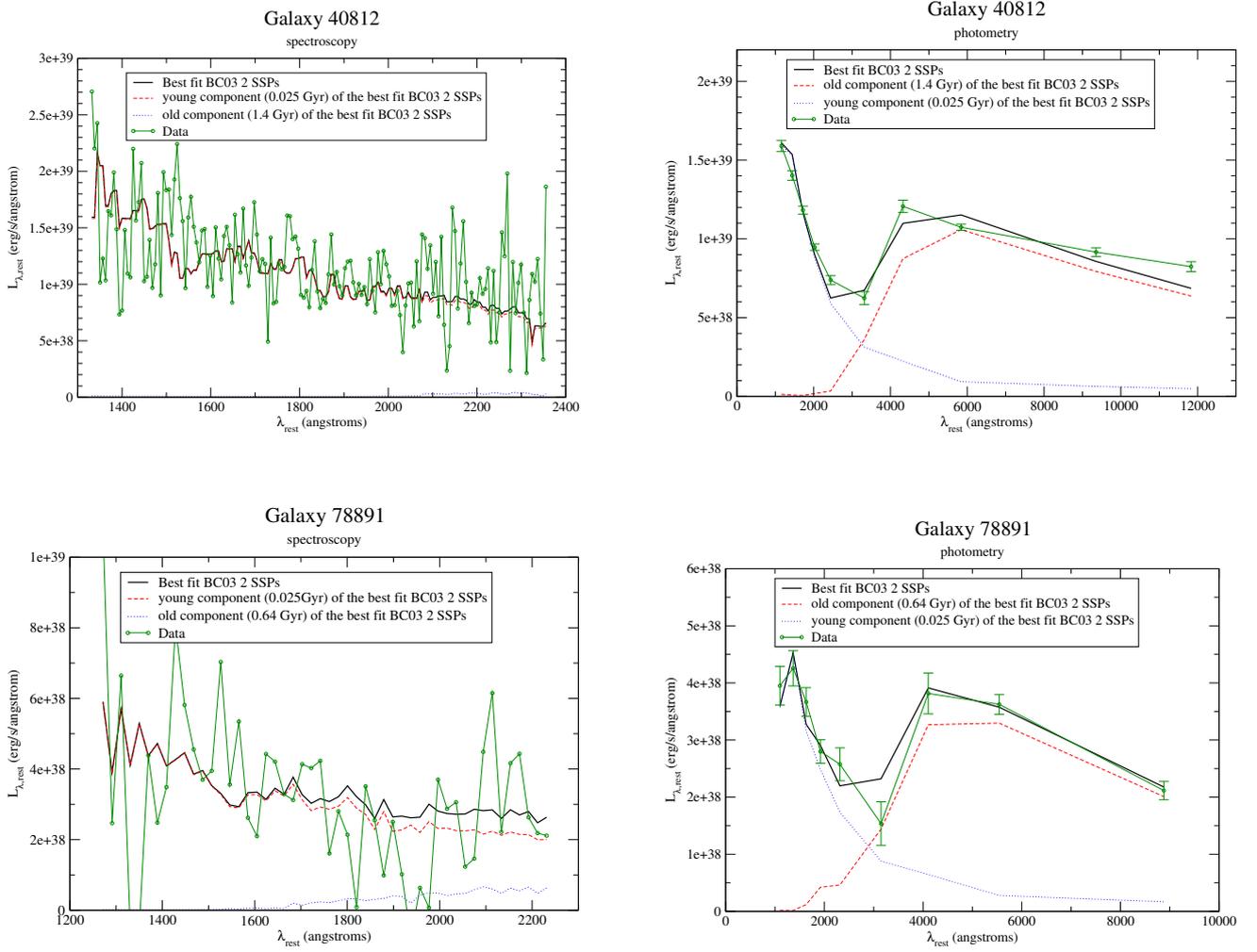
Fig. 6. Spectrum and photometry at rest corresponding to the best fits with two SSPs of BC03 model (see Table 2) of spectroscopy or photometry for galaxies #40812 and #78891, indicating the decomposition of the young and the old component.
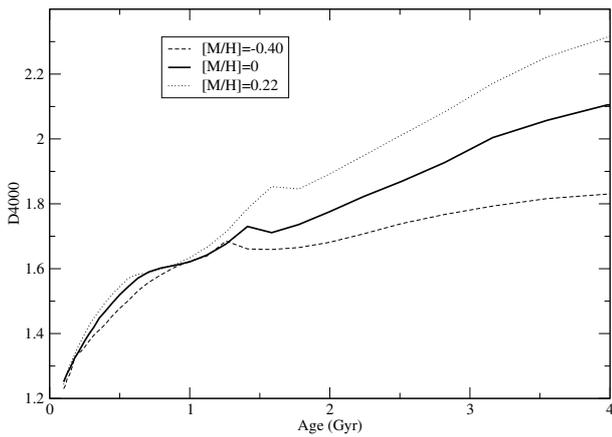

Fig. 7. Dependence of the Balmer break on the age and metallicity according to the E-MILES synthesis model.

means that by using the Balmer break in these cases and assuming a single population, we underestimate the age of the galaxy. Such uncertainties pose serious concerns on the reliability of the cosmic chronometer method, used to measure the Hubble parameter as a function of redshift, $H(z)$ (e.g., Moresco et al. 2012, 2016).

9. Conclusions

We present the results of fitting photometric data and spectra of two high redshift galaxies employing two different models of stellar populations. The fits of these two types of data with each of these models lead to age, metallicity, and redshift. These fits also show that the obtained spectra helped us to reach more constrained results, although it is possible to obtain similar estimates with higher errors based only on the photometric data. The number of points including spectra is much higher than the number of free parameters and the goodness of the best fit is more accurate. Furthermore, these spectra allowed us to conclude that a young population dominating the UV wavelengths is required since there is a lack of an abrupt break at 2000 Å at rest. Also, the spectra do not show any bump at 2175 Å characteristic of dust contribution, such as that of the Milky Way. However, we cannot discard the presence of dust contributions like small magellanic clouds or nearby starbursts (Calzetti et al. 2000).

Fig. 7); when we mix both populations with a ratio such that $F_{\lambda,\mathrm{old}}(4000\,\text{Å}) \approx F_{\lambda,\mathrm{young}}(4000\,\text{Å})$, we get an average $D_{4000} \approx 1.6$, corresponding to an average age of 0.8 Gyr (using E-MILES model; see Fig. 7), almost independent of the metallicity. This

Models of one SSP do not provide good fits to the photometric data. We find that combinations of several SSPs are required to simultaneously match both the blue and the red photometric data. Specifically, we require a dominant component with a very old population and a small stellar component of ∼100 Myr. Remarkably, the mass fraction contribution of the young component (<5%) is in good agreement with the results obtained by other authors when including the UV spectral range in nearby galaxies (e.g., Yi et al. 2011; Vazdekis et al. 2016). This is consistent with an in situ formation scenario with stellar population evolutions evolving passively. We have also tried to fit the data with an exponentially decaying star formation, giving significantly worse results than those achieved with two SSP fits. We note, however, that newer generations of cosmological hydrodynamical simulations like EAGLE tend to predict significantly larger star formation histories (Trayford et al. 2015). The young component of this double SSP is consistent with a residual star formation that can also be observed at lower redshift galaxies (e.g., Domínguez-Sánchez et al. 2016) and in the nearby Universe (e.g., Vazdekis et al. 1997; Atlee et al. 2009). This further shows the unprecedented sensitivity of the UV to the presence of such young contributions, even for objects at $z > 2$. The fits to most of the other galaxies in our sample, which were performed on the basis of their photometric data alone, also provide very similar results. Our fits favor a scenario where the vast majority of the stars of these extremely red objects formed rapidly, with these stellar populations ageing with time, although with small star formation events from accumulated residual gas.

CL12 gave an average age of 1–2 Gyr for the average population of these kinds of galaxies based on the relationship of $(B - V)_{\rm rest}$ assuming one SSP, and we see here that there are stars much older than that because we need at least two SSPs. We find that half of the galaxies of our sample have preferred best fits with ages of the oldest population larger than 3 Gyr, older than the Universe for the standard cosmological model at those obtained redshifts, but statistical and systematic errors due to the adopted assumptions erase this tension. Further research for these galaxies is necessary.

What is not uncertain and which constitutes the main solid result of this paper is the fact that one SSP cannot describe early type galaxies like the ones analyzed here. It represents a drawback in age estimator methods based on single lines or breaks, such as the Balmer break used in cosmic chronometers, thus invalidating the application of this technique to constrain the cosmological parameters.

References

Alcalde Pampliega, B., Pérez-González, P. G., Domínguez Sánchez, H., et al. 2015, in: Highlights of Spanish Astrophysics VIII, eds. A. J. Cenarro, F. Figueras, C. Hernández-Monteagudo, J. Trujillo Bueno, & L. Valdivielso, 360
Atlee, D. W., Assef, R. J., & Kochanek, C. S. 2009, ApJ, 694, 1539
Avni, Y. 1976, ApJ, 210, 642

Bedregal, A. G., Scarlata, C., Henry, A. L., et al. 2013, ApJ, 778, 126
Belli, S., Newman, A. B., & Ellis, R. S. 2015, ApJ, 799, 206
Bertelli, G., Bressan, A., Chiosi, C., Fagotto, F., & Nasi, E., 1994, A&AS, 106, 275
Bruzual, G. 2007, in Stellar Populations as Building Blocks of Galaxies, eds. A. Vazdekis, & R. Peletier (Cambridge: Cambridge Univ. Press), 125
Bruzual, G., & Charlot, S. 2003, MNRAS, 344, 1000 (BC03)
Calzetti, D., Armus, L., Bohlin, R. C., et al. 2000, ApJ, 533, 682
Castro-Rodríguez, N., & López-Corredoira, M. 2012, A&A, 537, A31 (CL12)
Chabrier, G. 2003, PASP, 115, 763
Cimatti, A., Daddi, E., Renzini, A., et al. 2004, Nature, 430, 184
Cimatti, A., Cassata, P., Pozzetti, L., et al. 2008, A&A, 482, 21
da Cunha, E., Charlot, S., & Elbaz, D. 2008, MNRAS, 388, 1595
Domínguez Sánchez, H., Pérez-González, P. G., Esquej, P., et al. 2016, MNRAS, 457, 3743
Fang, G.-W., Kong, X., & Wang, M. 2009, RA&A, 9, 59
Geier, S., Richard, J., Man, A. W. S., et al. 2013, ApJ, 777, 87
Guo, Q., White, S., Simon, B., et al. 2011, MNRAS, 413, 101
Gregg, M. D., Silva, D., Rayner, J., et al. 2006, in The 2005 HST calibration workshop: *Hubble* after the transition to two-gyro mode (NASA/CP2006-214134), eds. A. M. Koekemoer, P. Goudfrooij & L. L. Dressel, National Aeronautics and Space Administration, Goddard Space Flight Center, 209
Kaviraj, S., Schawinski, K., Devriendt, J. E. G., et al. 2007, ApJS, 173, 619
Koleva, M., & Vazdekis, A. 2012, A&A, 538, A143
La Barbera, F., Ferreras, I., Vazdekis, A., et al. 2013, MNRAS, 433, 3017
Labbé, I., Huang, J., Franx, M., et al. 2005, ApJ, 624, L81
Le Borgne, J.-F., Bruzual, G., Pelló, R., et al. 2003, A&A, 402, 433
Longhetti, M., Saracco, P., Severgnini, P., et al. 2005, MNRAS, 361, 897
Lonoce, I., Longhetti, M., Maraston, C., et al. 2015, MNRAS, 454, 3912
López-Corredoira, M. 2010, AJ, 139, 540
Maraston, C. 2005, MNRAS, 362, 799
McCarthy, P. J., Le Borgne, D., Crampton, D., et al. 2004, ApJ, 614, L9
Mendel, J. T., Saglia, R. P., Bender, R., et al. 2015, ApJ, 804, L4
Mignoli, M., Cimatti, A., Zamorani, G., et al. 2005, A&A, 437, 883
Moresco, M., Cimatti, A., Jiménez, R., et al. 2012, JCAP, 8, 6
Moresco, M., Pozzetti, L., Cimatti, A., et al. 2016, JCAP, 5, 14
Oke, J. B. 1990, AJ, 99, 1621
Onodera, M., Carollo, C. M., Renzini, A., et al. 2015, ApJ, 808, 161
Oser, L., Ostriker, J. P., Naab, T., Johansson, P. H., & Burkert, A. 2010, ApJ, 725, 2312
Pérez-González, P. G., Rieke, G. H., Villar, V., et al. 2008, ApJ, 675, 234
Pozzetti, L., & Mannucci, F. 2000, MNRAS, 317, L17
Renzini, A. 2006, ARA&A, 44, 141
Rodighiero, G., Cimatti, A., Franceschini, A., et al. 2007, A&A, 470, 21
Röck, B., Vazdekis, A., Ricciardelli, E., et al. 2016, A&A, 589, A73
Rowan-Robinson, M., Babbedge, T., Oliver, S., et al. 2008, MNRAS, 386, 697
Rowan-Robinson, M., González-Solares, E., Vaccari, M., & Marchetti, L. 2013, MNRAS, 428, 1958
Schiavon, R. P., Faber, S. M., Rose, J. A. & Castilho, B. V. 2002, ApJ, 580, 873
Schlafly, E. F., & Finkbeiner, D. P. 2011, ApJ, 737, 103
Simon, J. Verde, L., & Jiménez, R. 2005, Phys. Rev. D, 71, 123001
Steinhardt, C. L., Capak, P., Masters, D., & Speagle, J. S. 2016, ApJ, 824, 21
Taylor, E. N., Franx, M., van Dokkum, P. G., et al. 2009, ApJS, 183, 295
Tinsley, B. M. 1980, Fundamentals of Cosmic Physics, 5, 287
Toft, S., van Dokkum, P., Franx, M., et al. 2005, ApJ, 624, L9
Toft, S., Gallazzi, A., Zirm, A., et al. 2012, ApJ, 754, 3
Trayford, J. W., Theuns, T., Bower, R. G., et al. 2015, MNRAS, 452, 2879
Tremonti, C. 2003, Ph.D. Thesis, Johns Hopkins Univ., 766
Trujillo, I., Feulner, G., Goranova, Y., et al. 2006, MNRAS, 373, L36
van de Sande, J., Kriek, M., Franx, M., et al. 2013, ApJ, 771, 85
Vazdekis, A., Casuso, E., Peletier, R. F., & Beckman, J. E. 1996, ApJS, 106, 307
Vazdekis, A., Peletier, R. F., Beckman, J. E., & Casuso, E. 1997, ApJS, 111, 203
Vazdekis, A., Salaris, M., Arimoto, N. & Rose, J. A. 2001, ApJ, 549, 274
Vazdekis, A., Ricciardelli, E., Cenarro, A. J., et al. 2012, MNRAS, 424, 157
Vazdekis, A., Koleva, M., Ricciardelli, E., Röck, B., & Falcón-Barroso, J. 2016, MNRAS, 463, 3409
Whitaker, K. E., van Dokkum, P. G., Brammer, G., et al. 2013, ApJ, 770, L39
Wiklind, T., Dickinson, M., Ferguson, H. C., et al. 2008, ApJ, 686, 781
Williams, R. J., Quadri, R. F., Franx, M., van Dokkum, P., & Labbé, I. 2009, ApJ, 691, 1879
Yi, S. K., Lee, J., Sheen, Y.-K., et al. 2011, ApJS, 195, 22

Appendix A: Figures of the fit with two SSPs for the 18 galaxies of CL12, only with photometry
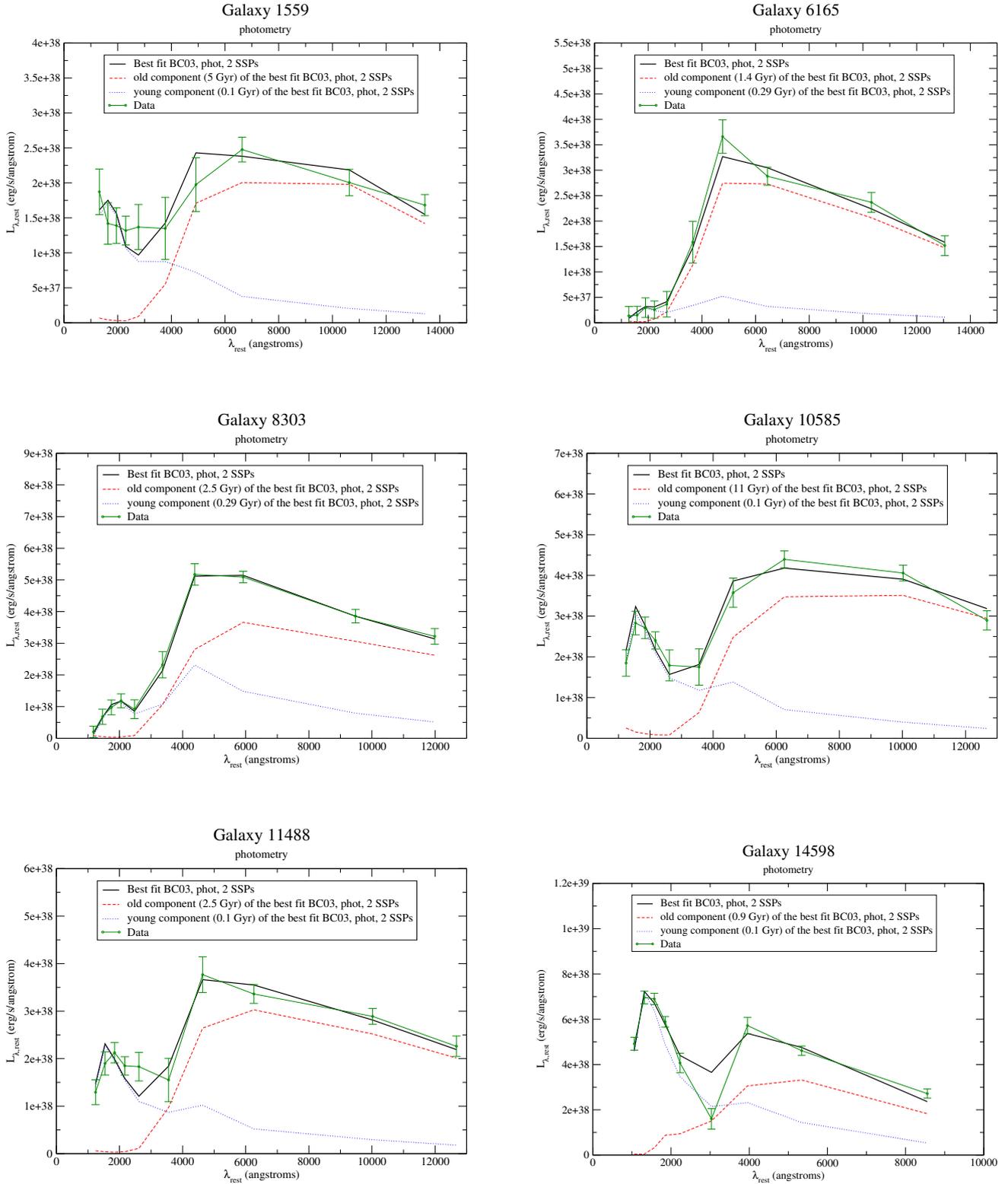

Fig. A.1. Photometry at rest corresponding to the best fits with two SSPs of BC03 model (see Table 3) for the CL12 galaxies, except #40812 and #78891.
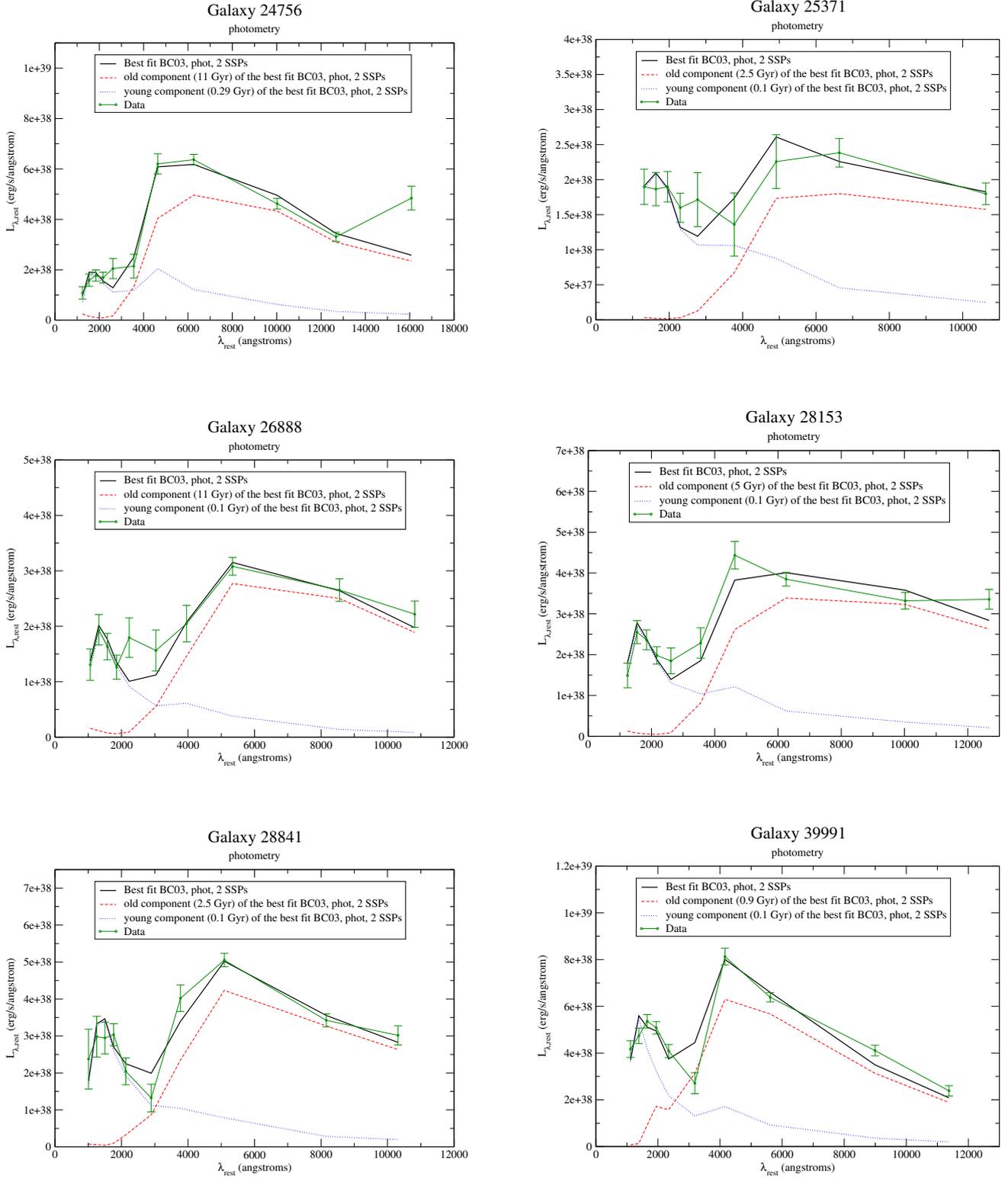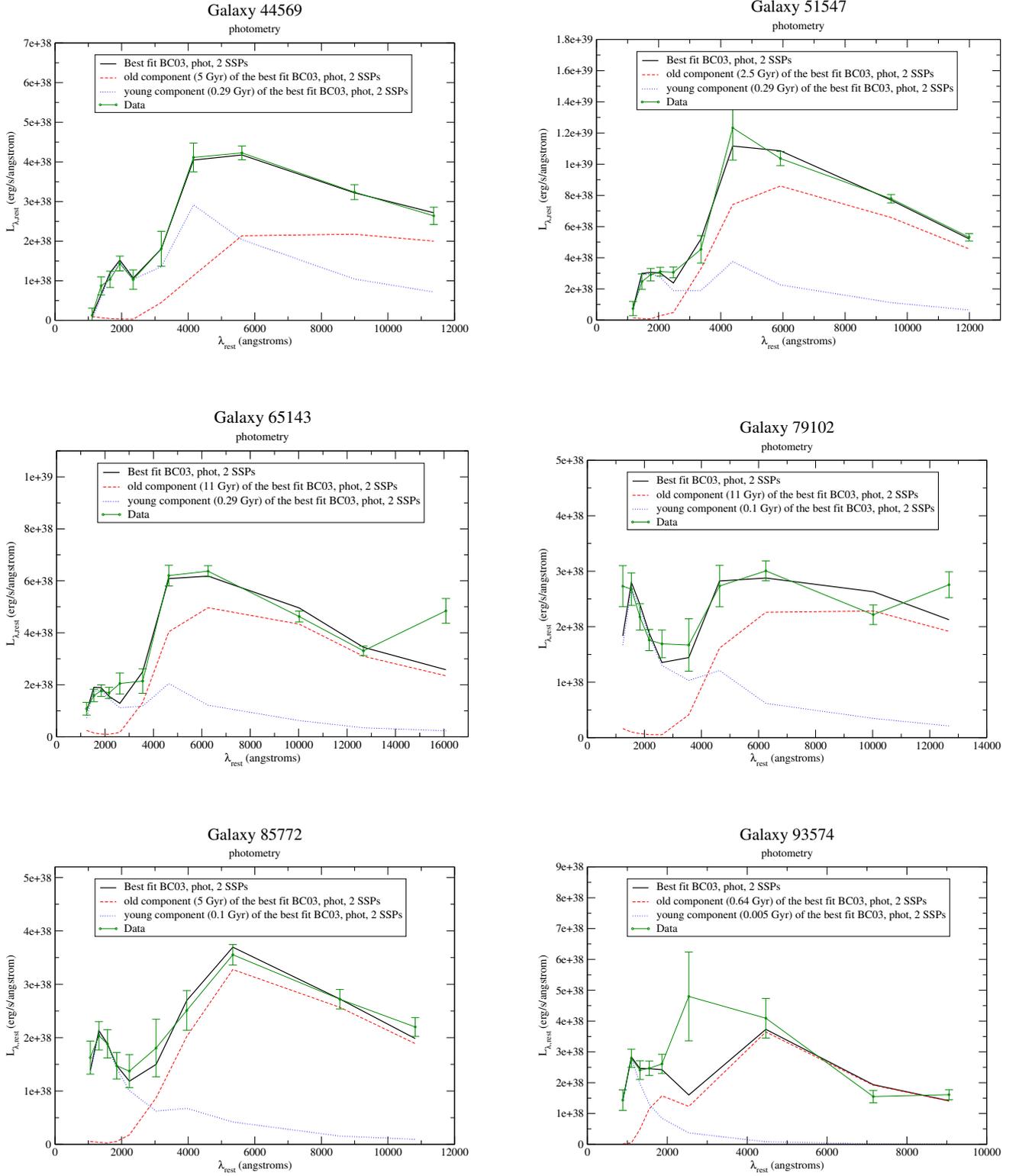
Galaxy 24756

Galaxy 25371

Galaxy 26888

Galaxy 28153

Galaxy 28841

Galaxy 39991

Fig. A.1. continued.

Galaxy 44569

photometry

Galaxy 51547

photometry

Galaxy 65143

photometry

Galaxy 79102

photometry

Galaxy 85772

photometry

Galaxy 93574

photometry

Fig. A.1. continued.